High magnetocaloric efficiency of a NiFe/NiCu/CoFe/MnIr multilayer in a small magnetic field

S. N. Vdovichev,[1] N. I. Polushkin,[1] I. D. Rodionov,[2] V. N. Prudnikov,[2] J. Chang,[3] and A. A. Fraerman[1]

[1]*Institute for Physics of Microstructures of RAS, GSP-105, Nizhny Novgorod, Russia*

[2]*Lomonosov Moscow State University, Faculty of Physics, Moscow 119991, Russia*

[3]*Center for Spintronics, Post-Si Semiconductor Institute, Korea Institute of Science and Technology, Hwarangno 14-gil 5, Seongbuk-gu, Seoul 02792, Korea*

(Received 18 January 2018; revised manuscript received 11 May 2018; published 26 July 2018)

The isothermal magnetic entropy changes ΔS (i.e., the magnetocaloric potential) are studied in $Ni_{80}Fe_{20}/Ni_{67}Cu_{33}/Co_{90}Fe_{10}/Mn_{80}Ir_{20}$ stacks at temperatures near the Curie point of the $Ni_{67}Cu_{33}$ spacer by applying magnetic fields of a few milli-Tesla. Such fields were sufficient for toggling magnetic moments in the soft ferromagnetic layer ($Ni_{80}Fe_{20}$). It is found that this switching provides a significant enhancement of ΔS in the heterostructure system with respect to that achieved in a single $Ni_{67}Cu_{33}$ film under such weak magnetic fields. Our finding is believed to have the potential to be utilized in magnetocaloric devices (e.g., thin-film coolers) that would be based on ferromagnetic/paramagnetic/ferromagnetic heterostructures and would operate with moderate magnetic fields.

DOI: 10.1103/PhysRevB.98.014428

I. INTRODUCTION

In materials that exhibit a strong magnetocaloric effect (MCE), high magnetocaloric efficiency can be achieved in the vicinity of phase magnetic transitions, e.g., near the Curie point (T_C) [1,2]. The MCE, observed currently in advanced magnetocaloric materials, is believed to be sufficient for cooling down (or heating up) the material by applying a magnetic field up to several Tesla over several tens of thermodynamic cycles [3–6]. However, such strong fields can only be produced with bulky magnets, which are not desirable to be employed in magnetic refrigeration [7]. Therefore, there have been attempts to find MCE materials in both their bulk and structured forms [7–12] that could be used for magnetic cooling under moderate fields. We propose to enhance the MCE by surrounding a magnetocaloric material by higher-T_C (strong) ferromagnets (FM's), [13,14] so that their reconfiguration in a weak enough field could affect magnetic moments in a paramagnetic (PM) spacer due to the effect of proximity [15]. It has been shown [14,16–19] that strong FM's surrounding a PM or a weakly FM spacer are exchange-coupled through the spacer, at least up to its thickness of ~20 nm [14].

Here we report on our measurements of the magnetic entropy changes ΔS (magnetocaloric potential) in $Ni_{80}Fe_{20}/Ni_{67}Cu_{33}/Co_{90}Fe_{10}/Mn_{80}Ir_{20}$ stacks at temperatures (T) close to T_C of the PM = $Ni_{67}Cu_{33}$ spacer between the strong FM layers, i.e., $FM_1 = Ni_{80}Fe_{20}$ and $FM_2 = Co_{90}Fe_{10}$. Such a heterostructure system exhibits reconfigurations of the mutual orientation of magnetizations $\mathbf{M}_1$ and $\mathbf{M}_2$ in the FM_1 and FM_2 layers under an applied field of $\mu_0 H_{sw} \sim 2$ mT due to their exchange decoupling across the spacer above T_C [16–19]. Our evaluations [13] of the MCE in FM/PM/FM structures anticipate a very high value of $dT/d(\mu_0 H) \approx 20$ K/T in bias fields of only a few milli-Tesla. As proposed in Refs. [13,14], this originates from demagnetization (magnetization) of the PM spacer when the mutual orientation of $\mathbf{M}_1$ and $\mathbf{M}_2$ alters from parallel (antiparallel) to antiparallel (parallel) alignment. Such a reconfiguration in a $FM_1/PM/FM_2/AF$ stack, where AF = $Mn_{80}Ir_{20}$ is the antiferromagnetic layer, is schematically shown in Fig. 1. The role of the AF layer is to render the FM_2 layer magnetically hard, which would contrast with the magnetically soft FM_1 layer. The dependence of ΔS on the mutual orientation of the magnetizations is associated with the giant MCE by analogy with the effect of giant magnetoresistance in spin valves [20,21]. It is also important that T_C of the spacer can be tunable by varying the spacer composition. For example, a diluted Ni_xCu_{1-x} alloy, whose T_C depends almost linearly on Ni concentration, is a good candidate for the spacer material [16–19].

II. SAMPLES PREPARATION AND CHARACTERIZATION

$FM_1/PM/FM_2/AF$ samples were fabricated with high-vacuum magnetron sputtering (AJA 2200 multichamber system) onto fused polished quartz substrates at a basic pressure of 10^{-5} Pa. To prevent them from oxidation, the samples were covered by a layer of TaO. The layers of $Ni_{80}Fe_{20}$ (FM_1), $Co_{90}Fe_{10}$ (FM_2), and $Mn_{80}Ir_{20}$ (AF) were sputtered from single targets, while PM films of Ni_xCu_{1-x} solid solutions were obtained by simultaneous sputtering of Ni and Cu targets, and their composition was determined by x-ray microanalysis using a dispersion spectrometer (INCA Energy Oxford Instruments). The exchange pinning between the FM_2 and AF layers was achieved during the film growth with the assistance of an in-plane magnetic field of $\mu_0 H \approx 200$ mT. Sample magnetization as a function of H was measured with a Lake Shore 7400 Series vibrating sample magnetometer and a MPMS-XL5 Quantum Design SQUID magnetometer in a 5–400 K temperature range and external magnetic fields up to $\mu_0 H = 0.5$ T applied in the film plane. The sample area used in these studies was $A = 0.2\,\mathrm{cm}^2$. The individual magnetizations of the strong FM layers, M_1 and M_2, were determined from the Kittel equation by measuring the ferromagnetic resonance

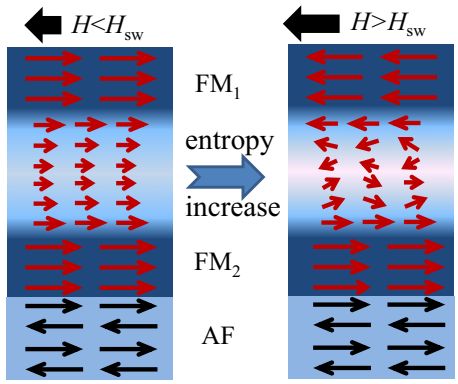

FIG. 1. Schematic of magnetic configurations in the $FM_1/PM/FM_2/AF$ heterostructure system, where AF is the antiferromagnet, whose role is to pin magnetic moments in the ferromagnet FM_2, while the FM_1 is magnetically soft. As magnetizations in the FM_1 and FM_2 layers are oriented in the same direction at $H < H_{sw}$, where H_{sw} is the switching field for magnetic moments in the soft layer, the PM spacer is magnetized (low magnetic entropy) by exchange coupling to the FM_1 and FM_2 across the interfaces. However, the PM spacer becomes demagnetized (high magnetic entropy) after switching of magnetization in the FM_1 layer at $H = H_{sw}$. In this thought experiment, the temperature is close to T_C of the PM spacer. In the geometry of antiparallel alignment ($H > H_{sw}$) of magnetic moments in the FM_1 and FM_2 layers, according to Eq. (A5), the magnetization becomes zero at the spacer center. This can be explained by thermal excitations of magnetic moments inside the spacer under such a configuration of the magnetizations. Under the parallel configuration ($H < H_{sw}$), magnetic moments inside the spacer are not thermally excited. Therefore, magnetization switching at $H = H_{sw}$ is expected to provide an enhanced magnetocaloric potential ΔS [13,14] by analogy with the effect of giant magnetoresistance [20,21].

[14]. The composition of the Ni_xCu_{1-x} solid solution was $x = 67$ at. %, while the thickness of the $Ni_{67}Cu_{33}$ spacer (h_{NiCu}) varied from 7 to 21 nm. The thickness of the soft $Ni_{80}Fe_{20}$ layer (FM_1) was $h_{NiFe} = (10 \pm 1)$ nm, and these quantities for the rest of the layers were as follows: 3.0 nm of $Co_{90}Fe_{10}$, 25 nm of $Mn_{80}Ir_{20}$, and 15 nm of TaO. The layer thicknesses were evaluated with small-angle x-ray diffraction data (reflectometry Bruker D8 Discover).

III. RESULTS AND DISCUSSION

Figure 2(a) shows the magnetization (M) isotherms, measured as the total magnetic moment $\mu \equiv MV$ of a $TaO/Mn_{80}Ir_{20}/Co_{90}Fe_{10}/(10\ nm)Ni_{67}Cu_{33}/Ni_{80}Fe_{20}$/substrate sample as a function of H, at temperatures of $T = 300$, 250, and 5 K. In the observed $M(H)$ dependences, we distinguish two steps that correspond to the switching of the soft (FM_1) and pinned (FM_2) layers. Importantly, the observed change in MV at the first (lower-H) step, which reflects switching of magnetic moments in both the FM_1 layer and $Ni_{67}Cu_{33}$ spacer (PM), is $A(2M_1h_{NiFe} + mh_{NiCu}) \approx 3.2 \times 10^{-7}$ A m^2, where m is the spacer magnetization. Retrieving the magnetization of the soft $Ni_{80}Fe_{20}$ layer $M_1 = 730$ kA/m from the ferromagnetic resonance data [14], we find that

$$2M_1h_{NiFe} >> mh_{NiCu}, \quad (1)$$

which is compatible with the expected smallness of magnetization in the PM spacer by comparison to that in the FM surrounding. The observed delay in the switching of magnetization in the FM_2 layer results from the exchange coupling of magnetic moments across the FM_2/AF interface. We also see that the field H_{sw} at which magnetization ($\mathbf{M}_1$) in the FM_1 layer is switchable increases upon lowering T. Therefore, reversal of $\mathbf{M}_1$ becomes undistinguishable from that of $\mathbf{M}_2$ of the FM_2 layer at low enough $T < 100$ K.

In Fig. 2(b) we show H_{sw} versus T near $T_C \approx 240$ K of $Ni_{67}Cu_{33}$ [22] for the samples with 10- and 21-nm-thick $Ni_{67}Cu_{33}$ spacers. The fact that H_{sw} depends on T indicates that exchange through the spacer is sensitive to the temperature. Indeed, reversal of $\mathbf{M}_1$ occurs at $H_{sw} = JM_2$ [23], where JM_2 is the effective magnetic field acting on the FM_1 layer from the FM_2 layer pinned by the AF, and J is the interlayer exchange constant, which depends on T [17]. Also, the $J(T)$ dependence—with its derivation in the explicit form—is

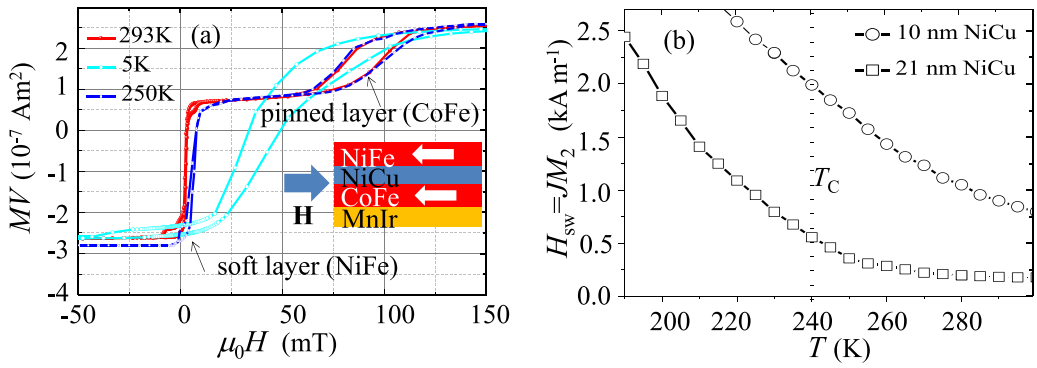

FIG. 2. (a) Isothermal magnetization of a $TaO/Mn_{80}Ir_{20}/Co_{90}Fe_{10}/(10\ nm)Ni_{67}Cu_{33}/Ni_{80}Fe_{20}$/substrate sample at temperatures of $T = 300$, 250, and 5 K. In the response to an applied magnetic field ($\mu_0 H$), the magnetization reversal occurs in two steps that correspond to magnetization switching in the soft ($FM_1 = Ni_{80}Fe_{20}$) and pinned ($FM_2 = Co_{90}Fe_{10}$) layers. Reversal of magnetization in the FM_2 layer is delayed due to exchange coupling of magnetic moments in this layer with those in the antiferromagnetic layer ($AF = Mn_{80}Ir_{20}$) across the FM_2/AF interface. The inset illustrates the mutual configuration of an applied field $\mathbf{H}$ and magnetizations in the FM_1 and FM_2 layers before switching of magnetization in the soft FM_1 layer, which occurs at $H = H_{sw}$. (b) The switching field $H_{sw} = J(T)M_2$ [23] measured as a function of temperature T for 10- and 21-nm-thick $Ni_{67}Cu_{33}$ spacers.

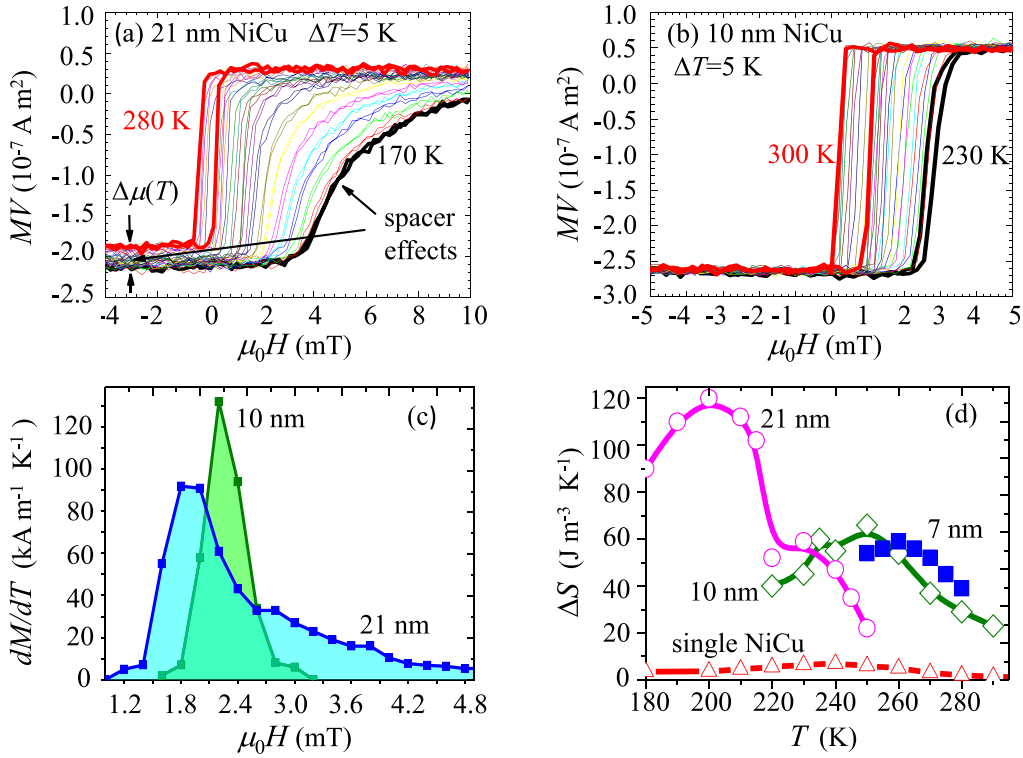

FIG. 3. (a),(b) Reversal of magnetization in the soft FM_1 layer under an applied magnetic field H at different T. The $M(H)$ curves were taken for the samples with 21 nm (a) and 10 nm (b) $Ni_{67}Cu_{33}$ spacers in temperature ranges of 280–170 and 300–230 K with steps of 5 K. The spacer effects on $M(H)$ are clearly pronounced in the sample with the thicker spacer. (c) $\partial M/\partial T$-vs-H curves for the samples with 10 and 21 nm spacers at $T = 250$ and 210 K, respectively, at which ΔS are maximal. (d) $\Delta S(T)$ curves evaluated by integration according to Eq. (2) for the samples with spacers of different thicknesses − 7, 10, and 21 nm. Obtained values of ΔS for the heterostructure samples are compared to that quantity in a single $Ni_{67}Cu_{33}$ film, which is retrievable by extrapolation into the low-field region ($\mu_0 H \sim 2.0$ mT) of the experimental $\Delta S(T)$ dependences measured at high $\mu_0 H \geqslant 1$ T and presented in Ref. [22].

discussed in the Appendix. We do not mark a large difference between H_{sw} as functions of T for samples with different thicknesses of the spacer.

Figures 3(a) and 3(b) show in greater detail how the soft ferromagnet (FM_1) switches in the samples with 21-nm-thick (a) and 10-nm-thick (b) spacers. These data were collected in temperature ranges of 280–170 and 300–230 K with steps of $\Delta T = 5$ K. A magnetic field **H** was applied along the direction antiparallel to that of $\mathbf{M}_1$ and $\mathbf{M}_2$ in their initial configuration [inset in Fig. 2(a)]. We have found that the magnetic response in both samples depends strongly on T under H in a few mT. Strikingly, in the sample with a thicker spacer, there is a contribution of the spacer to $M(H)$, that is, the increase in saturation magnetization with lowering T, which is indicated in Fig. 3(a) by $\Delta\mu$ that depends on T. Moreover, a much more gradual switching of the FM_1 in this sample, which depends on T in a relatively broad field range (up to $\mu_0 H \sim 5$ mT), can also be attributed to the spacer effect. Switching of the FM_1 in the sample with a thinner spacer occurs in a much sharper manner [Fig. 3(b)]. The spacer contribution to $M(H,T)$ is expected to provide the magnetocaloric potential, which can be accounted for in accordance with the Maxwell relation

$$\Delta S = \mu_0 \int_{H_{sw}-\varepsilon_1}^{H_{sw}+\varepsilon_2} \left(\frac{\partial M}{\partial T}\right)_H dH. \qquad (2)$$

The $\partial M/\partial T$-H data, required for accounting for ΔS, were obtained by plotting the $M(T)$ and their numerical differentiation within a field range of $[H_{sw} - \varepsilon_1;\ H_{sw} + \varepsilon_2]$ inside of which $(\partial M/\partial T)_H \neq 0$. The $\partial M/\partial T$-versus-H curves are shown in Fig. 3(c) for the samples with 10- and 21-nm-thick spacers at temperatures $T = 250$ and 210 K, which provide the largest values of ΔS in accordance with Eq. (2). It is interesting that the $\partial M/\partial T$-versus-H curves are asymmetric functions with respect to H_{sw}, at which $\partial M/\partial T$ are maximal. It is seen that this asymmetry is much stronger in the sample with a thicker spacer where the spacer effects on the switching of the FM_1 are more pronounced. Because of exchange coupling at the FM_1/PM interface, thermally unstable magnetic moments inside the PM spacer intervene in the switching of the FM_1, which becomes more gradual upon thickening the spacer [Fig. 3(a)]. Therefore, the spacer contribution to ΔS is distinguishable: The more pronounced the asymmetry is in the dependence of $\partial M/\partial T$ on H, the higher is ΔS.

Figure 3(d) shows $\Delta S(T)$ dependences for the samples with 7-, 10-, and 21-nm-thick spacers. The magnetocaloric potential retrieved in the heterostructure samples can be compared to that quantity in a single $Ni_{67}Cu_{33}$ film exposed by a magnetic field of $\mu_0 H \sim 2$ mT. The values of ΔS in such weak fields for $Ni_{67}Cu_{33}$ were found by extrapolation into the low-field region of the $\Delta S(H) \propto H^n$ dependences [24] with $n \approx 0.8$ at T close to $T_C \approx 240$ K of $Ni_{67}Cu_{33}$, which have been reported

in Ref. [22]. Although the maximal peak values of $\partial M/\partial T$ are obtained to be highest for the sample with a thinner (10 nm) spacer [Fig. 3(c)], we mark that $\Delta S \approx 120\,\mathrm{J/m^3\,K}$ is higher in the sample with a relatively thick (21 nm) spacer [Fig. 3(d)]. Strikingly, the maximal ΔS obtained in the heterostructure samples is up to ~20 times larger than that in a single $Ni_{67}Cu_{33}$ film. Such a change in the magnetic entropy is expected to provide the adiabatic cooling of the refrigerant $\Delta T_{ad} = -(T/C_V)\Delta S \approx -0.006\,\mathrm{K}$, taking into account that the heat capacity increases near T_C, so that $C_V \approx 5.0\,\mathrm{J/cm^3K}$ [26]. Note here that the magnetocaloric efficiency in the system under study is $\partial T/\partial(\mu_0 H) = -(T/C_H)(\partial M/\partial T) \sim -5\,\mathrm{K/T}$, which is comparable to this quantity in advanced magnetocaloric materials [1,2].

It is also interesting that the magnetocaloric potential for the heterostructure system we study can also be evaluated as

$$\Delta S = 2\mu_0 (dJ/dT) M_1 M_2, \tag{3}$$

which is obtainable by substituting $M = M_1 \mathrm{sgn}(H_{eff})$ [23] into Eq. (2). Having measured $H_{sw}(T)$ [Fig. 2(b)], we find that the highest $dJ/dT = (dH_{sw}/dT)/M_2 = 4.0 \times 10^{-5}\,\mathrm{K^{-1}}$ [25] is achievable for the sample with a thick (21 nm) spacer at $T \approx 210$ K [Fig. 2(b)], where the ΔS is largest. We see that Eq. (3) provides a simple relationship between ΔS and intrinsic properties of the spacer.

The observed enhancement of ΔS reflects the occurrence of stronger disorder in magnetic moments inside a thick enough spacer under the antiparallel configuration of $\mathbf{M}_1$ and $\mathbf{M}_2$. To qualitatively explain this central feature of our work, we schematically show (Fig. 4) the isothermal magnetization of the $FM_1/PM/FM_2/AF$ system as a function of H for two temperatures T_1 and T_2, so that $T_1 > T_2$ and thus $J(T_1) < J(T_2)$. If, for instance, the system stays in the state A at T_1, lowering the temperature down to T_2 provides a transition of the system to the state B, with a strongly different magnetization, as indicated by the arrow. This transition results from the switching of $\mathbf{M}_1$, which provides the redistribution of magnetic moments in the spacer. We emphasize here that, in the geometry of antiparallel alignment of $\mathbf{M}_1$ and $\mathbf{M}_2$ (state A), magnetization at the center of the PM spacer is zero; see Eq. (A5). This results from thermal excitations of magnetic moments in the PM spacer under such a configuration of $\mathbf{M}_1$ and $\mathbf{M}_2$ (Fig. 1). However, the parallel configuration of $\mathbf{M}_1$ and $\mathbf{M}_2$ (state B) provides a higher thermal stability of magnetic moments in the spacer. Therefore, a switching of $\mathbf{M}_1$ can provide the change in magnetic entropy. A temperature range within which the transition from state A to B occurs is defined by the efficiency of the interlayer exchange as a function of T, i.e., by dJ/dT. The change of the magnetic moment under varying T occurs within a finite field range, $J(T_1)M_2 < H < J(T_2)M_2$. With increasing a bias field $H > H_{sw}$, $\partial M/\partial T$ quickly decays [Fig. 3(b)]. This imposes a constraint for the adiabatic temperature change (ΔT_{ad}) per one switching of $\mathbf{M}_1$. If a bias field is small, $H < H_{sw}$, there is no change in the magnetic entropy at all.

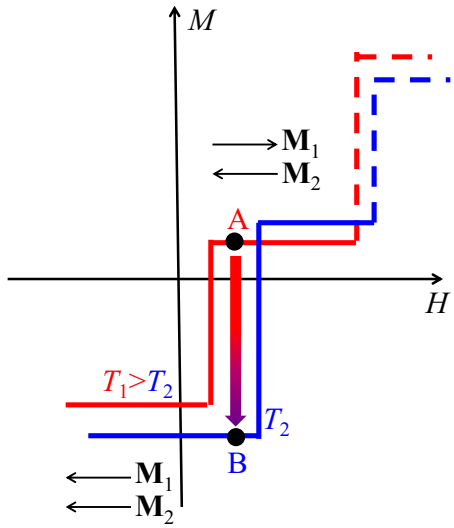

FIG. 4. Schematic of the $M(H)$ dependence for an $FM_1/PM/FM_2/AF$ heterostructure system at two temperatures, T_1 and T_2. The transition of the system from the state A (antiparallel orientation of magnetizations $\mathbf{M}_1$ and $\mathbf{M}_2$) to the state B (parallel orientation of the magnetizations $\mathbf{M}_1$ and $\mathbf{M}_2$) is triggered by lowering the temperature from T_1 to T_2. The switching between the A and B states provides the redistribution of magnetization inside the spacer and thus the change in magnetic entropy.

IV. CONCLUSION

We show that, at temperatures close to T_C of the $Ni_{67}Cu_{33}$ spacer, $Ni_{80}Fe_{20}/Ni_{67}Cu_{33}/Co_{90}Fe_{10}/Mn_{80}Ir_{20}$ multilayers exhibit the magnetocaloric potential ΔS, which is much higher than that in a single $Ni_{67}Cu_{33}$ paramagnet under weak magnetic fields (a few milli-Tesla). The changes in magnetic entropy occur upon the magnetic-field-driven reconfiguration of the soft FM ($Ni_{80}Fe_{20}$) with respect to the pinned one ($Co_{90}Fe_{10}$). Magnetization switching in the $Ni_{80}Fe_{20}$ layer affects the distribution of magnetic moments in the spacer [16–19], which leads to the enhancement of ΔS [13]. In this article, we present experimental evidence that the spacer is indeed responsible for this enhancement. To theoretically treat the observed changes in ΔS when altering the spacer thickness, the calculation of ΔS presented in Ref. [13] as well as the theoretical model for the interlayer exchange presented in the Appendix should be elaborated upon further. It is also important that the experimental data obtained are interpretable in a frame of a simple phenomenological model [16–19], which uncovers the relationship [Eq. (3)] between ΔS and the spacer property, i.e., the temperature derivative of the interlayer exchange constant.

ACKNOWLEDGMENTS

Work was supported by the Russian Foundation for Basic Research (project No. 17-0200620_a) and by the Program of Fundamental Research of the Presidium of the Russian Academy of Sciences "Nanostructures: Physics, Chemistry, Biology, Technology Basics." The authors thank P. Yunin and S. Gusev for their assistance in studying the structural properties of the samples. J. C. acknowledges the support of the KIST Institutional Program (2E27140).

APPENDIX: SIMPLIFIED MODEL FOR INTERLAYER COUPLING

Here we derive the equation for the interlayer exchange constant and show that it is sensitive to the temperature. To describe the interlayer coupling through the PM spacer, we write the free energy per area unit [13,14]:

$$\frac{F_s}{\mu_0} = \int_{|z|<h/2} \left[\frac{1}{2}\alpha^2 \left(\frac{\partial \mathbf{m}}{\partial z} \right)^2 + \frac{1}{2}\tau \mathbf{m}^2 + \frac{1}{4m^2}\mathbf{m}^4 \right] dz + \frac{1}{2} l(\mathbf{M}_1 - \mathbf{m})^2 \Big|_{z=+h/2} + \frac{1}{2} l(\mathbf{M}_2 - \mathbf{m})^2 \Big|_{z=-h/2}, \tag{A1}$$

where the region $-h/2 < z < h/2$ is occupied by a spacer with magnetization $\mathbf{m}(z)$ and is surrounded from both sides at $z = \pm h/2$ by strong FM's with magnetizations $\mathbf{M}_1$ and $\mathbf{M}_2$ for simplicity, having equal saturation magnetizations $M_1 = M_2 \equiv M$ with the components of $(M\cos\vartheta/2, \pm M\sin\vartheta/2, 0)$, ϑ is the angle between magnetizations of the strong FM's, $\tau = (T - T_C)/T_C$, $\alpha \approx (k_B T_C/am_0^2)^{1/2}$ is the effective exchange length, a is the interatomic distance, and m_0 is the saturation magnetization of the spacer. The first term in Eq. (A1) is the free energy of the spacer, which is written in the form of the Landau expansion. The second and third terms reflect the exchange with the strong FM's that surround the PM spacer, in which l is the exchange constant at the interfaces.

The equation that gives extreme(s) of the functional in Eq. (A1) reads

$$\alpha^2 \frac{\partial^2 \mathbf{m}}{\partial z^2} - \tau \mathbf{m} - \frac{\mathbf{m}^3}{m_0^2} = 0, \tag{A2}$$

while the boundary conditions at the interfaces are as follows:

$$\alpha^2 \frac{\partial \mathbf{m}}{\partial z} = \pm l(\mathbf{M}_{1,2} - \mathbf{m})|_{z=\pm h/2}. \tag{A3}$$

Finding $\mathbf{m}(z)$ by solving the system of Eqs. (A2) and (A3) and substitution of the obtained solution into Eq. (A1) should allow one to clarify how the interlayer exchange depends on different parameters, e.g., ϑ, T, and h. Within an approximation of the weak exchange at the interfaces, i.e., $l << h\tau$ and $lh << \alpha^2$, one can discard the nonlinear term in Eq. (A2), so that the solution could be found in its analytic form. Then, the magnetization components in the spacer can be written as

$$m_x = \frac{lM\cos(\vartheta/2)}{\alpha\sqrt{\tau}\sinh(h/2\xi) + \xi\cosh(h/2\xi)} \cosh(z/\xi), \quad -h/2 < z < h/2; \tag{A4}$$

$$m_y = \frac{lM\sin(\vartheta/2)}{\alpha\sqrt{\tau}\cosh(h/2\xi) + \xi\sinh(h/2\xi)} \sinh(z/\xi), \quad -h/2 < z < h/2; \tag{A5}$$

where $\xi = \alpha/\sqrt{\tau}$ is the correlation length in the spacer. The spacer magnetization essentially depends on h/ξ. If the spacer is thick enough ($h/\xi >> 1$), the coupling between the strong FM's through the spacer exponentially approaches zero. In the opposite case of a thin spacer ($h/\xi << 1$) and within an approximation of the weak interfacial exchange, we get that

$$\frac{F_s}{\mu_0} = -\frac{3l^2M^2}{h\tau}\cos\vartheta. \tag{A6}$$

Thus, our calculations indicate that the free energy of our system can be presented in the Heisenberg-like form, i.e., $F_s = -\mu_0 J_l \mathbf{M}_1\mathbf{M}_2$, where $J_l = 3l^2/h\tau$ is the interlayer exchange constant obtained in units of length. As expected, the effective interlayer coupling depends on temperature as $\propto (T - T_C)^{-1}$ at T close to T_C.

[1] A. M. Tishin and Y. I. Spichkin, *The Magnetocaloric Effect and Its Application* (IOP, Bristol, 2003).

[2] A. Gschneidner Jr., V. K. Pecharsky, and A. O Tsokol, Recent developments in magnetocaloric materials, Rep. Prog. Phys. **68**, 1479 (2005).

[3] U. Tomc, J. Tusek, A. Kitanovski, and A. Poredos, A new magnetocaloric refrigeration principle with solid-state thermoelectric thermal diodes, Appl. Therm. Eng. **58**, 1 (2013).

[4] W. Vries and Th. H. van der Meer, Application of Peltier thermal diodes in a magnetocaloric heat pump, Appl. Therm. Eng. **111**, 377 (2017).

[5] B. Monfared, Simulation of solid-state magnetocaloric refrigeration systems with Peltier elements as thermal diodes, Int. J. Refrigeration **74**, 324 (2017).

[6] T. Tsukamoto, M. Esashi, and S. Tanaka, Magnetocaloric cooling of a thermally-isolated microstructure, J. Micromech. Microeng. **22**, 094008 (2012).

[7] T. Mukherjee, S. Sahoo, R. Skomski, D. J. Sellmyer, and Ch. Binek, Magnetocaloric properties of Co/Cr superlattices, Phys. Rev. B **79**, 144406 (2009).

[8] R. Skomski, C. Binek, T. Mukherjee, S. Sahoo, and D. J. Sellmyer, Temperature- and field-induced entropy changes in nanomagnets, J. Appl. Phys. **103**, 07B329 (2008).

[9] V. Franco, K. R. Pirota, V. M. Prida, A. M. J. C. Neto, A. Conde, M. Knobel, B. Hernando, and M. Vazquez, Tailoring of magnetocaloric response in nanostructured materials: Role of anisotropy, Phys. Rev. B **77**, 104434 (2008).

[10] C. W. Miller, D. D. Belyea, and B. J. Kirby, Magnetocaloric effect in nanoscale thin films and heterostructures, J. Vac. Sci. Technol. A **32**, 040802 (2014).

[11] Y. Liu, L. C. Phillips, R. Mattana, M. Bibes, A. Barthélémy, and B. Dkhil, Large reversible caloric effect in FeRh thin films via a dual-stimulus multicaloric effect in FeRh thin films via a dual-stimulus multicaloric cycle, Nat. Commun. **7**, 11614 (2016).

[12] V. V. Khovaylo, V. V. Rodionova, S. N. Shevyrtalov, and V. Novosad, Magnetocaloric effect in "reduced" dimensions: Thin films, ribbons, and microwires of Heusler alloys and related compounds, Phys. Status Solidi B **251**, 2104 (2014).

[13] A. A. Fraerman and I. A. Shereshevskii, Magnetocaloric effect in ferromagnet/paramagnet multilayer structures, JETP Lett. **101**, 618 (2015).

[14] E. V. Skorokhodov, E. S. Demidov, S. N. Vdovichev, and A. A. Fraerman, Ferromagnetic resonance in a system of magnetic films with different Curie temperatures, J. Exp. Theor. Phys. **124**, 617 (2017).

[15] D. Schwenk, F. Fishman, and F. Schwabl, Ferromagnetic multilayers: Statics and dynamics, Phys. Rev. B **38**, 11618 (1988).

[16] A. F. Kravets, A. N. Timoshevskii, B. Z. Yanchitsky, M. A. Bergmann, J. Buhler, S. Andersson, and V. Korenivski, Temperature-controlled interlayer exchange coupling in strong/weak ferromagnetic multilayers: A thermomagnetic Curie switch, Phys. Rev. B **86**, 214413 (2012).

[17] A. F. Kravets, Y. I. Dzhezherya, A. I. Tovstolytkin, I. M. Kozak, A. Gryschuk, Y. O. Savina, V. A. Paschenko, S. L. Gnatchecnko, B. Koop, and V. Korenivski, Synthetic ferrimagnets with thermomagnetic switching, Phys. Rev. B **90**, 104427 (2014).

[18] A. F. Kravets, D. M. Polishchuk, Y. I. Dzhezherya, A. I. Tovstolytkin, V. O. Golub, and V. Korenivski, Anisotropic magnetization relaxation in ferromagnetic multilayers with variable interlayer exchange coupling, Phys. Rev. B **94**, 064429 (2016).

[19] A. F. Kravets, A. I. Tovstolytkin, Y. I. Dzhezherya *et al.*, Spin dynamics in a Curie-switch, J. Phys.: Condens. Matter **27**, 446003 (2015).

[20] G. Binasch, P. Grunberg, F. Saurenbach, and W. Zinn, Enhanced magnetoresistance in layered magnetic structures with antiferromagnetic interlayer exchange, Phys. Rev. B **39**, 4828 (1989).

[21] M. N. Baibich, J. M. Broto, A. Fert, F. Nguyen Van Dau, F. Petroff, P. Etienne, G. Creuzet, A. Friederich, and J. Chazelas, Giant magnetoresistance of (001)Fe/(001)Cr magnetic superlattices, Phys. Rev. Lett. **61**, 2472 (1988).

[22] S. Michalski, R. Skomski, X.-Zh. Li, D. Le Roy, T. Mukherjee, Ch. Binek, and D. J. Sellmyer, Isothermal entropy changes in nanocomposite Co:$Ni_{67}Cu_{33}$, J. Appl. Phys. **111**, 07A930 (2012).

[23] An external magnetic field **H** is applied in the film plane and aligned to the easy axis of the uniaxial magnetic anisotropy. Neglecting the latter quantity, the magnetic free-energy density is $F/\mu_0 = -J(T)\mathbf{M}_1\mathbf{M}_2 - \mathbf{M}_1\mathbf{H} = -MH_{\text{eff}}$, where $M = M_1\text{sgn}(H_{\text{eff}})$ and $H_{\text{eff}} = -J(T)M_2 + H$. By definition, the magnetic entropy can be found as $S = -\partial F/dT$, so that $\partial S/\partial(\mu_0 H) = -\partial^2 F/\partial T\partial(\mu_0 H)$. Taking into account that $(dJ/dT)M_2(\partial M/\partial H) = \partial M/\partial T$, integration of $\partial S/\partial(\mu_0 H)$ on H between $H = H_{\text{sw}} + \varepsilon_2$ and $H = H_{\text{sw}} - \varepsilon_1$ leads to Eq. (2).

[24] V. Franco, J. S. Blázquez, and A. Conde, Field dependence of the magnetocaloric effect in materials with a second order phase transition: A master curve for the magnetic entropy change, Appl. Phys. Lett. **89**, 222512 (2006).

[25] Similarly to M_1, the quantity of M_2 was obtained from the ferromagnetic resonance data as well; see Ref. [14].

[26] K. E. Grew, The specific heat of nickel and of some nickel-copper alloys, Proc. R. Soc. London, Ser. A **145**, 509 (1934).